*J. Phys. Chem. Solids* Pergamon Press 1958. Vol. 7. pp. 1–13.

# THE PREPARATION, CRYSTALLOGRAPHY, AND MAGNETIC PROPERTIES OF THE $Li_xCo_{(1-x)}O$ SYSTEM

**W. D. JOHNSTON, R. R. HEIKES and D. SESTRICH**

Westinghouse Research Laboratories, Pittsburgh 35, Pennsylvania

(*Received* 27 *January* 1958; *revised* 3 *March* 1958)

**Abstract**—The $Li_xCo_{(1-x)}O$ system has been prepared by the solid-state reaction between $Li_2O_2$ and CoO at 900°C. The material is a single-phase structure in the composition range $0 < x < 0{\cdot}2$, the lattice parameter of the cubic unit cell decreasing with increasing lithium content. At the composition $x = 0{\cdot}5$ (i.e. $LiCoO_2$) a rhombohedral structure is formed. A phase diagram for this system has been developed.

The crystal structure of material in the composition range $0 < x < 0{\cdot}2$ has been studied both above and below the antiferromagnetic Curie temperature. Both the antiferromagnetic Curie temperature and the related cubic–tetragonal transformation are found to occur at decreasing temperatures with increasing lithium content. In addition the magnitude of the crystallographic deformation decreases and finally vanishes with increasing lithium content.

The magnetic-susceptibility data indicate that the magnetic moment of $Co^{+2}$ is best understood if the multiplet splitting is small compared to $kT$. Further, the moment of $Co^{+3}$ is shown to be lowered by crystalline field effects. No effects attributable to the double exchange coupling were found. The absence of such a coupling is understood by consideration of the mechanism of electron transfer in the lithium-substituted compounds.

## 1. INTRODUCTION

In a recent paper[1] the preparation, structural evaluation, and magnetic properties of the $Li_xMn_{(1-x)}O$ system have been reported. The present paper describes some of the subsequent studies made on the analogous system $Li_xCo_{(1-x)}O$. This system has been prepared through the use of the method originally devised for $Li_xMn_{(1-x)}O$. The products have been studied both crystallographically and magnetically. The electrical properties of this system as well as those of the $Li_xMn_{(1-x)}O$, $Li_xNi_{(1-x)}O$ and $Li_xCu_{(1-x)}O$ systems have been previously reported.[2]

One of the reasons for initiating work on the lithium-substituted transition-metal oxides was the desire to gain a further understanding of the double-exchange interaction. This is an indirect interaction which is expected to occur between like ions in different valence states in crystallographically equivalent sites. Such an interaction was first proposed by ZENER[3] in order to understand the occurrence of ferromagnetism and metallic-type electrical conductivity in some substituted perovskites, e.g. $La_xSr_{(1-x)}MnO_3$. It was expected that the introduction of lithium into the divalent transition-metal oxides might induce ferromagnetism due to the formation of mixed valence states on equivalent sites. As has been reported previously,[1] no evidence for ferromagnetism was found in the $Li_xMn_{(1-x)}O$ system. To obtain further information as to the possibility of ferromagnetism in this type of system, the magnetic properties of $Li_xCo_{(1-x)}O$ were examined in detail.

The parent compound of this system, CoO, is antiferromagnetic. Many antiferromagnetic substances are known to have symmetry changes at the Curie point.[4,5] An interpretation of these symmetry changes was first given by GREENWALD and SMART[6] in terms of an "exchange-type magnetostriction". For example, neutron-diffraction experiments on NiO indicate that (111) planes are ferromagnetic, while the direction of magnetization alternates in going along the [111] direction. SMART postulated that the exchange interaction between neighboring (111) planes caused the observed rhombohedral distortion.



RJ Technology Exhibit 2034
Apple Inc. v. RJ Technology LLC
IPR2023-01183, Page 1 of 13

However, in the case of CoO, to which SHULL[7] assigned the same spin structure as NiO, a tetragonal distortion is found experimentally. LI[8] attempted to resolve this situation by a reinterpretation of SHULL's results. However, recent work[9–11] indicates that the axis of easy magnetization in these oxides is [111] instead of [100] as needed in LI's theory and as proposed originally by SHULL.[7] Apparently the issue is not yet settled, as ROTH[12] has shown that multispin-axis arrangements are to be preferred from single-crystal data.

The effect of foreign-ion substitution on the distortion in NiO was noted by SHIMOMURA.[13] He found that copper lessened the distortion while aluminum increased it. Further, he found that at high copper concentrations the material remained cubic even below the antiferromagnetic Curie temperature, $T_c$. BROWNLEE and MITCHELL[14] reported the qualitative observation that the rhombohedral deformation is less in $Li_xNi_{(1-x)}O$ than in pure NiO.

In the present work a detailed crystallographic study has been made of the structural changes which occur in the $Li_xCo_{(1-x)}O$ system below the antiferromagnetic Curie temperature. These results are discussed in connection with the magnetic data.

## 2. EXPERIMENTAL

### (a) *Preparation*

Cobalt oxide was prepared by dissolving Fisher nickel-free cobalt in concentrated nitric acid, filtering the solution, and then evaporating to dryness. The material, after heating in air to drive off all nitrous fumes, yielded a black oxide. This oxide was placed in a platinum crucible and was heated in air for 3 hr at 400° and 14 hr at 900°. It was finally heated for 14 hr at 1100°C in a pumped vacuum. The product was reddish-brown in color.

This material was analyzed spectroscopically for alkali-metal impurities. The results (in p.p.m.) are Na 1–10, Li < 10, K < 50, Rb < 100, and Cs < 500.

The preparation of $Li_2O_2$ has been previously described.[1] The preparation of samples in the $Li_xCo_{(1-x)}O$ system as well as for certain samples in the $Li_xNi_{(1-x)}O$ and $Li_xCu_{(1-x)}O$ system was performed as previously described for the $Li_xMn_{(1-x)}O$ system.[1] The divalent transition-metal oxide and $Li_2O_2$ were mixed and pressed into pellets under an argon atmosphere. The pellets were then fired for 24 hr in a sealed container of small volume, and finally quenched. By this method it was possible to prepare pure single-phase samples in the composition ranges CoO–$Li_{0.2}Co_{0.8}O$, NiO–$Li_{0.15}Ni_{0.85}O$, and CuO–$Li_{0.02}Cu_{0.98}O$. The products containing 1 atomic per cent lithium or more were black in color. The mechanical strength of the pellets has been observed to decrease in the order Mn > Co > Ni > > Cu. In the case of the $Li_xCo_{(1-x)}O$ system the upper limit of lithium concentration is due to the existence of a phase boundary in the system. On the other hand samples in the $Li_xNi_{(1-x)}O$ and $Li_xCu_{(1-x)}O$ systems containing more than the maximum amount of lithium indicated above attacked their platinum containers during the sintering reaction and resulted in samples of doubtful purity. It should be emphasized, however, that the maximum lithium concentrations in these two cases do not correspond to phase boundaries. Samples containing less than the limiting lithium contents for the various systems appear to be relatively free from platinum contamination. Spectroscopic analysis of these materials indicate less than 100 p.p.m. of platinum.

Analytical data for samples in the $Li_xCo_{(1-x)}O$ system are given in Table 1. In these materials it was impossible to correct the sample composition for loss by volatilization of $Li_2O$ in the same manner as was done in the case of $Li_xMn_{(1-x)}O$,[1] since there is considerable fragmentation of these pellets during preparation. This made any correction on the basis of weight loss of very doubtful accuracy. It will be noted from the analytical data that there is little need for such a correction.

Lithium was determined either gravimetrically as the sulfate or through the use of a flame photometer. Oxidizing power was measured by dissolving the sample in ferrous ammonium sulfate under argon and then titrating with ceric sulfate or potassium dichromate. The result is recorded as trivalent metal. Cobalt metal was determined by electro-deposition.

$LiCoO_2$, which occurs when $x = 0{\cdot}5$ in the general formula $Li_xCo_{(1-x)}O$, was prepared by both the present method as well as by a previously reported method[15] in which $Li_2CO_3$ is reacted with $CoCO_3$ in air at 900–1000°C. The two methods

RJ Technology Exhibit 2034
Apple Inc. v. RJ Technology LLC
IPR2023-01183, Page 2 of 13

*Table* 1. *Analytical data*

| Composition | Wt.-% Lithium | | Wt.-% $Co^{+3}$ | | Wt.-% Co Total | | At.-% $Li^{+1}$ / At.-% $Co^{+3}$ |
|---|---|---|---|---|---|---|---|
| | Calculated | Found | Calculated | Found | Calculated | Found | |
| CoO | | | 0·00 | 0·16 | 78·6 | 78·4 | |
| $Li_{0·01}Co_{0·99}O$ | 0·093 | 0·098 | 0·79 | 0·72 | 78·4 | 78·4 | 1·04 |
| $Li_{0·05}Co_{0·95}O$ | 0·48 | 0·42 | 4·1 | 3·6 | 77·4 | 78·4 | 1·00 |
| $Li_{0·08}Co_{0·92}O$ | 0·78 | 0·70 | 6·7 | 5·9 | 76·6 | 77·8 | 1·00 |
| $Li_{0·10}Co_{0·90}O$ | 1·00 | 0·90 | 8·4 | 7·6 | 76·1 | 77·1 | 1·01 |
| | | 0·93 | | 7·8 | | 77·3 | 1·02 |
| $Li_{0·15}Co_{0·85}O$ | 1·55 | 1·46 | 13·2 | 12·6 | 74·6 | 77·1 | 0·98 |
| $Li_{0·20}Co_{0·80}O$ | 2·15 | 2·26 | 18·3 | 18·9 | 73·1 | 75·2 | 1·02 |
| $Li_{0·25}Co_{0·75}O$ | 2·80 | 2·89 | 23·8 | 23·9 | 71·4 | 74·0 | 1·03 |
| $Li_{0·30}Co_{0·70}O$ | 3·50 | 3·45 | 29·8 | 28·9 | 69·5 | 70·8 | 1·01 |
| $Li_{0·35}Co_{0·65}O$ | 4·28 | 4·24 | 36·4 | 35·5 | 67·5 | 66·3 | 1·01 |
| $Li_{0·50}Co_{0·50}O$ | 7·09 | 7·37 | 60·2 | 59·3 | 60·2 | 61·3 | 1·05 |

yield the same product according to their X-ray patterns.

(b) *X-ray studies*

Much of the X-ray examination was carried out as previously described.[1] The samples were all ground and X-rayed as a mineral-oil mull in order to prevent reaction with the air. Cobalt radiation, $\lambda K\alpha_1$ and $\lambda K\alpha_2$ having wavelengths 1·78892 and 1·79278 Å, respectively, was used. In the single-phase regions, all X-ray patterns were sharp, indicating that the samples were homogeneous.

The structure of $LiCoO_2$ was indexed from the powder pattern obtained with an 11·54-cm-diameter Debye camera. The density was determined pycnometrically, using toluene. Integrated intensities were obtained with a North American Philips proportional counter unit. These data are given in Table 2. In several cases intensity data are recorded for lines which were too faint to be measured on the Debye film. The highest-angle line measured on the Debye film could not be scanned with the proportional counter and thus no intensity data are recorded.

Low-temperature X-ray measurements were made using the bottom of a 19-cm Unicam high-temperature camera. A rotating-anode X-ray tube, designed and built by Dr. A. TAYLOR of this laboratory, was employed and permitted exposures to be taken in ½–1 hr, which considerably simplified the temperature-control problem. The sample was cooled by a stream of cold nitrogen gas impinging on it from above. The cold nitrogen gas was produced by energizing an electric heater submerged in a Dewar of liquid nitrogen. This gas was conducted to the sample through thermally insulated tubing. The rate of the gas stream, which determined the sample temperature, was controlled by manually varying the power input to the electric heater. Temperature was measured by a thermocouple placed within ⅛ in. of the sample. Calibration showed that this thermocouple gave a true reading of sample temperature. A tube, concentric with the nitrogen gas jet, supplied a stream of dry air to the area to prevent frost formation. The concentric tubes both ended with 1-in. long Cellophane tubes which surrounded the sample and through which X-rays could readily pass. With this rather simple apparatus, temperatures could be held constant to within several degrees in the temperature range studied, −130 to +25°C.

The accuracy of these measurements is approximately ±2 parts in 10,000 and is somewhat less than would be expected for a 19-cm camera for the following reasons. First, the line splitting which was studied in this work was rather slight and often somewhat diffuse, making measurement difficult. In some cases only one split line (420) was measurable. Secondly, in the experimental set-up used, sample eccentricity was sometimes a problem. In a few cases where this effect was noted, it was minimized by using $\cos^2\theta$ as an extrapolation function

RJ Technology Exhibit 2034
Apple Inc. v. RJ Technology LLC
IPR2023-01183, Page 3 of 13

*Table 2. X-ray diffraction data for* $LiCoO_2$

Space group $R\bar{3}m - D_{3d}^5$
Hexagonal axes $a = 2{\cdot}8166$ Å
$c = 14{\cdot}052$ Å
Density calculated 5·16 g/cc.
Density found 5·05 g/cc.
Atomic co-ordinates
$(000; \frac{1}{3}\frac{2}{3}\frac{2}{3}; \frac{2}{3}\frac{1}{3}\frac{1}{3}) +$
Co 3*a*: 000
Li 3*b* $00,\frac{1}{2}$
O 3*c* $00z$, $00z$
$z = 0{\cdot}26$

| *hkl* | $\sin^2\Theta$ converted to Co$\lambda$K$\alpha$ | | *F* | | $I_{obs}$ |
|---|---|---|---|---|---|
| | Obs. | Calc. | Obs. | Calc. | |
| 003 | 0·0366 | 0·0365 | 71·8 | 63·1 | 1068 |
| 101 | 0·1388 | 0·1387 | 46·4 | 42·0 | 163 |
| 006 | 0·1453 | 0·1461 | 26·6 | 24·1 | 32 |
| 012 | 0·1511 | 0·1509 | 24·0 | 21·8 | 48 |
| 104 | 0·1998 | 0·1996 | 82·5 | 76·0 | 377 |
| 015 | 0·2361 | 0·2361 | 33·7 | 31·4 | 56 |
| 009 | — | 0·3287 | 33·1 | 31·7 | 14 |
| 107 | 0·3333 | 0·3335 | 47·5 | 45·5 | 92 |
| 018 | 0·3946 | 0·3943 | 61·8 | 60·3 | 116 |
| 110 | 0·4041 | 0·4040 | 64·1 | 62·7 | 86 |
| 113 | 0·4407 | 0·4409 | 41·2 | 40·7 | 60 |
| 10,10 | 0·5417 | 0·5404 | 26·6 | 27·1 | 20 |
| 021 | 0·5436 | 0·5427 | 30·4 | 30·9 | 19 |
| 116 | 0·5499 | 0·5500 | 24·4 | 24·9 | 23 |
| 202 | — | 0·5549 | 19·7 | 23·8 | 9 |
| 00,12 | 0·5851 | 0·5843 | 48·0 | 49·5 | 28 |
| 024 | 0·6040 | 0·6036 | 50·6 | 52·4 | 49 |
| 01,11 | 0·6264 | 0·6256 | 38·1 | 39·7 | 40 |
| 205 | 0·6398 | 0·6401 | 24·5 | 25·7 | 13 |
| 119 | 0·7332 | 0·7327 | 19·9 | 21·4 | 21 |
| 027 | 0·7382 | 0·7375 | 31·5 | 34·0 | 32 |
| 208 | $\alpha_1$0·7985 | 0·7983 | 40·7 | 44·6 | 56 |
| | $\alpha_2$0·7990 | | | | |
| 10,13 | 0·8205 | 0·8204 | 16·5 | 18·2 | 13 |
| 00,15 | $\alpha_1$0·9128 | 0·9130 | 31·8 | 36·0 | 32 |
| | $\alpha_2$0·9127 | | | | |
| 01,14 | $\alpha_1$0·9300 | 0·9299 | 21·4 | 24·4 | 26 |
| | $\alpha_2$0·9296 | | | | |
| 02,10 | 0·9444 | 0·9441 | 17·1 | 19·6 | 22 |
| 211 | 0·9468 | 0·9470 | 22·1 | 25·3 | 45 |
| 122 | $\alpha_1$0·9589 | 0·9591 | 16·9 | 19·4 | 38 |
| | $\alpha_2$0·9587 | | | | |
| 11,12 | $\alpha_1$0·9880 | 0·9892 | — | — | — |
| | $\alpha_2$0·9878 | | | | |

instead of the more general function of Taylor and Sinclair (ref. in KLUG and ALEXANDER.[16]

(c) *Phase diagrams*

Data from which a phase diagram for $Li_xCo_{(1-x)}O$ was derived are given in Table 3. In order to demonstrate that equilibrium was attained, samples were prepared in such a manner that equilibrium was approached from two directions. One approach to equilibrium involves reacting

RJ Technology Exhibit 2034
Apple Inc. v. RJ Technology LLC
IPR2023-01183, Page 4 of 13

*Table 3. X-ray data for phase diagram (Original composition* $= Li_{0.3}Co_{0.7}O$)

| Sample heat-treatment (°C) | Lattice parameter of cubic phase (Å) | Composition of cubic phase |
|---|---|---|
| Prep. 900°, anneal 600° | 4·244 | $Li_{0.045}Co_{0.955}O$ |
| Prep. 650° | 4·239 | $Li_{0.060}Co_{0.940}O$ |
| Prep. 650° | 4·236 | $Li_{0.065}Co_{0.935}O$ |
| Prep. 700° | 4·212 | $Li_{0.125}Co_{0.875}O$ |
| Prep. 900°, anneal 700° | 4·216 | $Li_{0.115}Co_{0.885}O$ |
| Prep. 900°, anneal 750° | 4·206 | $Li_{0.14}Co_{0.86}O$ |
| Prep. 760° | 4·206 | $Li_{0.14}Co_{0.86}O$ |
| Prep. 810° | 4·185 | $Li_{0.185}Co_{0.815}O$ |
| Prep. 900°, anneal 850° | 4·174 | $Li_{0.210}Co_{0.790}O$ |

CoO and $Li_2O_2$ for at least 20 hr at the temperature being studied. The other involves preparing the $Li_xCo_{(1-x)}O$ material at a high temperature, 900°C, and then annealing for at least 20 hr at the proper lower temperature. The agreement of the data obtained by these two methods indicates that equilibrium has been achieved. All lines in the X-ray patterns of the products in the two-phase region are accounted for on the basis of the NaCl and $CsCl_2I$ structures. The composition of the NaCl phase of $Li_xCo_{(1-x)}O$ in the two-phase mixtures was obtained by comparing the lattice parameter of this phase with a plot of lattice parameter versus composition.

The $LiCoO_2$ phase shown on the diagram is believed to have a negligible range of solid solution. The *c*-axis of its hexagonal unit cell is independent of annealing temperature in the two-phase region, while the *a*-axis changes from that of the stoichiometric material by a maximum of only 5 parts in 10,000 at very low temperatures. The change of volume of the cell is negligible when compared with the change in volume versus composition of the phase with the rock-salt structure and would suggest a change in $x$ of only 0·0025. Admittedly such an analysis is far from rigorous, but it is believed to give a qualitatively correct result.

(d) *Magnetic measurements*

The gradient method used in making the magnetic measurements has been previously described.[1] Samples were contained in small sealed Vycor bulbs to prevent reaction with the atmosphere during magnetic testing.

## 3. DISCUSSION

(a) *Preparation*

The system $Li_xCo_{(1-x)}O$, as well as $Li_xNi_{(1-x)}O$ and $Li_xCu_{(1-x)}O$, has been successfully prepared by the method originally devised for the preparation of $Li_xMn_{(1-x)}O$,[1] indicating that the following reaction between $Li_2O_2$ and a divalent transition-metal oxide is a general one for the preparation of lithium-substituted transition-metal oxides.

$$\frac{x}{2}Li_2O_2+(1-x)MO \rightarrow Li_xM_{(1-x)}O$$
$$\equiv Li_x^{+}M_x^{+3}M_{(1-2x)}^{+2}O^{=}.$$

The compositions of the products in the $Li_xCo_{(1-x)}O$ system are probably best indicated by the ratio of atomic per cent $Li^+$ to oxidizing power (which is recorded as $Co^{+3}$). As can be seen from the above formula, such a ratio should equal unity. Table 1 shows that the experimental ratios are very close to this value.

(b) *X-ray study*

The values of the X-ray lattice parameter versus composition for $Li_xCo_{(1-x)}O$ are plotted on Fig. 1 with our corresponding data for $Li_xNi_{(1-x)}O$ included for comparison. In both cases there is a decrease in cell dimensions with increased lithium content. This decrease in the $Li_xCo_{(1-x)}O$ system is due to a twofold effect. First, $Li^+$ is smaller than $Co^{+2}$, and secondly, the $Co^{+3}$ formed is smaller than either $Li^+$ or $Co^{+2}$. In the $Li_xNi_{(1-x)}O$ system the decrease in lattice parameter with lithium content is not as pronounced, since $Li^+$ and $Ni^{+2}$ are

RJ Technology Exhibit 2034
Apple Inc. v. RJ Technology LLC
IPR2023-01183, Page 5 of 13

more nearly equal in size and thus the change in the cell dimension will be primarily due to the smaller size of the $Ni^{+3}$ formed. The introduction of small amounts of lithium into the tenorite lattice of CuO causes only a very small decrease in lattice spacing.

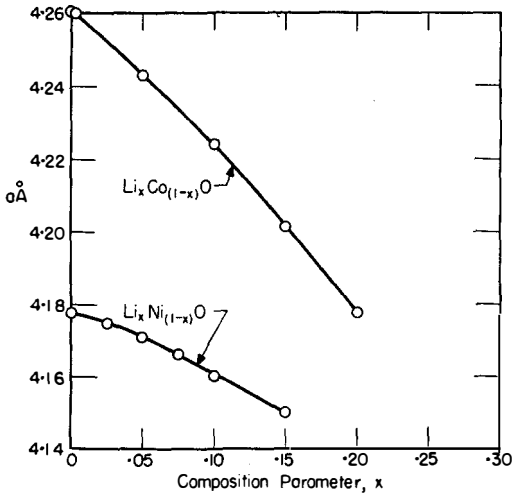


FIG. 1. X-ray lattice parameter of NaCl phase of $Li_xCo_{(1-x)}O$ and $Li_xNi_{(1-x)}O$ versus composition.

Samples of $Li_xCo_{(1-x)}O$ having values of $x$ near 0·5 gave a new X-ray pattern. These lines were indexed and the material was found to be $LiCoO_2$, having a rhombohedral $CsCl_2I$ structure. The hexagonal cell contains three formula weights. This structure has recently been reported by BONGERS.[17] Such a structure has also been reported for the similar compound $LiNiO_2$.[18] The cell dimensions given in Table 2 are referred to hexagonal axes. These values are in agreement with those of BONGERS, who gives $a = 2{\cdot}81$ and $c = 14{\cdot}0$ Å. The intensity data for $LiCoO_2$ give the best agreement with the calculated data with an oxygen parameter $z = 0{\cdot}26$. With this parameter the agreement index or residual as defined by

$$R = \frac{\Sigma \big| |F_0| - |F_c| \big|}{\Sigma |F_0|},$$

where $F_0$ and $F_c$ are the observed and calculated structure factors, is found to be 0·11. The corresponding values for $z = 0{\cdot}25$ and $z = 0{\cdot}27$ are 0·19 and 0·16, respectively. The calculated values of $F_c$ in the table have been corrected for the effect of temperature. It may be noted that in all cases the (00$l$) reflections are much stronger than the calculated values. This suggests either a preferred orientation of the sample crystallites or that the atomic scattering factors are markedly anisotropic.

Each $Co^{+3}$ or $Li^{+1}$ ion in the crystal is surrounded by a distorted octahedron of oxygen with the cobalt–oxygen distance about 8 per cent smaller than the lithium–oxygen distance. The cobalt–oxygen distance is also somewhat smaller than the nickel–oxygen distance in $LiNiO_2$, where $z$ was found to have a value of 0·25. There is little difference between the lithium–oxygen distances of the two compounds.

### (c) *Phase diagram*

After the characterization of the $LiCoO_2$ phase was completed, it became possible to examine the phase diagram of the $Li_xCo_{(1-x)}O$ system in the range $0 \leqslant x \leqslant 0{\cdot}5$. It seemed possible that this system might have a phase diagram similar to that found for $Li_xMn_{(1-x)}O$. The diagram for this system (Fig. 2) shows that the phase having the

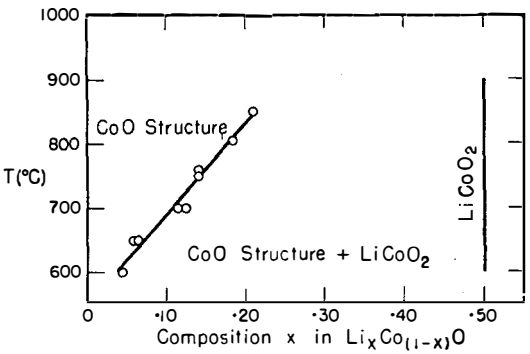


FIG. 2. Phase diagram for $Li_xCo_{(1-x)}O$.

rock-salt structure which has been studied here is actually a high-temperature phase. The transformation from the phase with NaCl structure to the lower-temperature two-phase mixture is slow enough that by quenching preparations from 900° the high-temperature phase can be retained. In none of the cases where samples were quenched from 900° and in which $x < 0{\cdot}2$ was any line of the $LiCoO_2$ phase observed in the X-ray pattern. The lines of the phase with rock-salt structure were

RJ Technology Exhibit 2034
Apple Inc. v. RJ Technology LLC
IPR2023-01183, Page 6 of 13

always sharp. Further, the samples prepared in this manner are quite stable and do not transform at moderate temperatures. This behavior is exactly what was observed in the $Li_xMn_{(1-x)}O$ system. Thus, in both cases pure samples of the high-temperature phase can be readily prepared and retained by the normal preparation procedure.

(d) *Low-temperature X-ray study*

As pointed out earlier, pure antiferromagnetic oxides such as MnO, CoO, and NiO undergo structural modifications at their antiferromagnetic Curie temperature as a result of magnetic ordering. In order to examine this effect more closely, a study was made of both the magnetic susceptibility and the structural transformation of the $Li_xCo_{(1-x)}O$ system. This system was chosen for study first because the antiferromagnetic Curie temperature is located at a convenient temperature, room temperature, and secondly because the deformation in pure CoO has been thoroughly studied.[4]

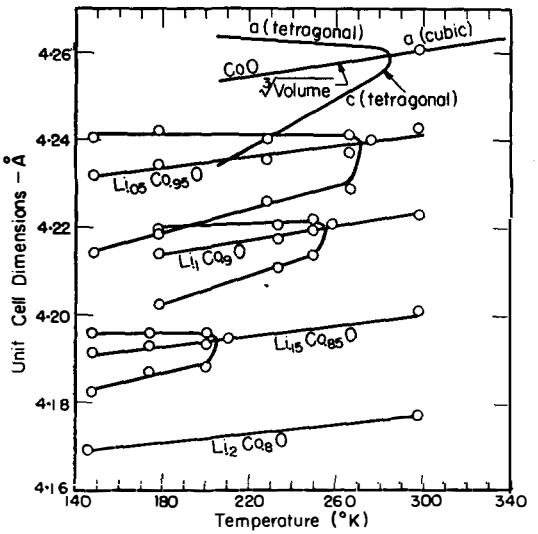


FIG. 3. Unit cell dimensions for $Li_xCo_{(1-x)}O$ versus temperature.

The low-temperature crystal-structure data for the $Li_xCo_{(1-x)}O$ system are graphically shown in Fig. 3. GREENWALD's data on pure CoO are included for comparison. In all but one case a crystallographic distortion to tetragonal symmetry occurs as the temperature is lowered, with the parameter $a$ increasing slightly and $c$ decreasing. The cube root of volume (which, of course, is equal to $a$ in the cubic case) is linear throughout. The distortion to tetragonal is always quite abrupt. One of the most significant features of these data is that the temperature at which the distortion occurs decreases with increased lithium content. With the exception of $Li_{0.2}Co_{0.8}O$, the temperature of this crystallographic distortion is in relatively good agreement with the antiferromagnetic Curie temperature obtained from susceptibility measurements, as can be seen in Fig. 4. Secondly, the

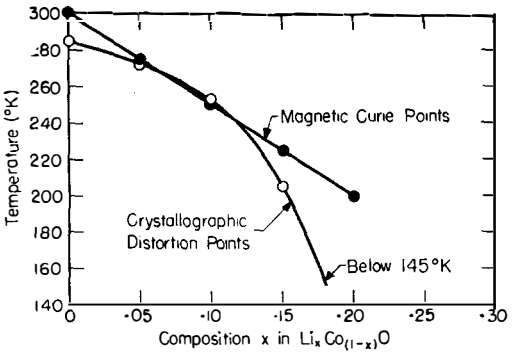


FIG. 4. Antiferromagnetic Curie points and crystallographic distortion points versus composition $x$ in $Li_xCo_{(1-x)}O$.

amount of crystallographic distortion generally decreases with increased lithium concentration. Both this decrease in the deformation temperature and the decrease in the amount of distortion are in agreement with what would be expected on the basis of a decreased magnetic coupling due to the dilution of the cobalt ions. In $Li_{0.2}Co_{0.8}O$ sufficient lithium has entered the lattice to suppress the transformation, as the data show that 55° below $T_c$ there is no structural distortion. It is impossible to say whether the structural distortion is completely eliminated in this material, whether it is too small to be observed, or whether it is moved to a much lower temperature.

The abrupt nature of the deformation at constant lithium content as the temperature is decreased has been previously noted. In addition it should be pointed out that the deformation is also abrupt as lithium content is varied at constant temperature. A three-dimensional plot summarizing these data is presented in Fig. 5. In this plot the

RJ Technology Exhibit 2034
Apple Inc. v. RJ Technology LLC
IPR2023-01183, Page 7 of 13

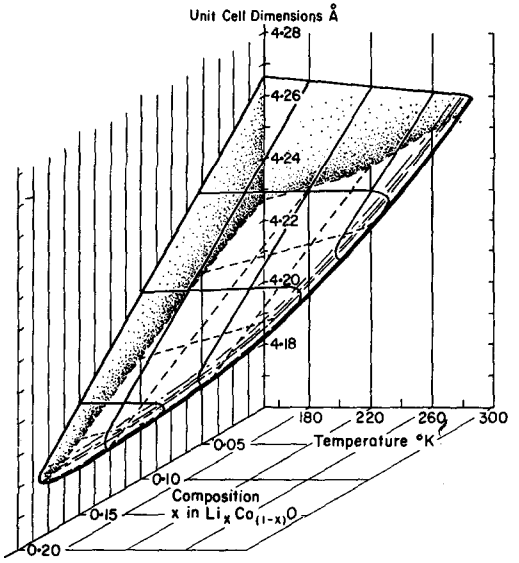


FIG. 5. Surface showing X-ray lattice parameters of $Li_xCo_{(1-x)}O$ as a function of composition and temperature.

amount of distortion in the antiferromagnetic range is given as a function of both temperature and composition. This plot emphasizes the equivalent roles of temperature and composition in defining the distortion region and also illustrates the abrupt nature of the onset of the crystallographic deformation.

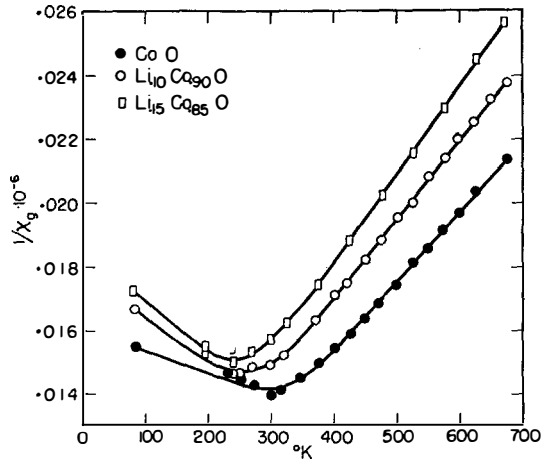


FIG. 6. Reciprocal susceptibility versus absolute temperature for $Li_xCo_{(1-x)}O$.

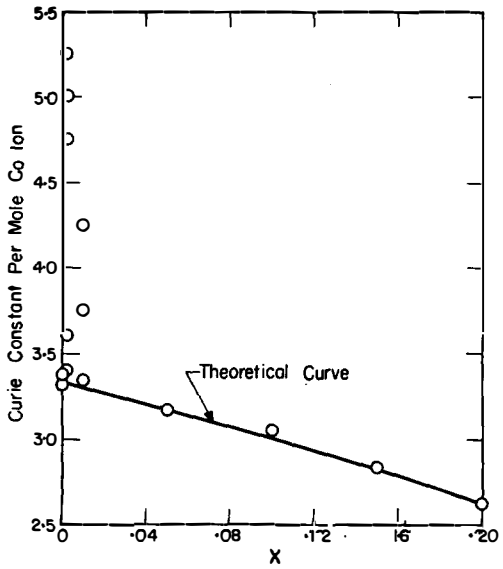


FIG. 7. Curie constant versus mole fraction of lithium.

(e) *Magnetism*

The experimental magnetic data will now be examined to determine the magnitude of the magnetic moments of the ions and the magnitude of the various interactions. The situation with regard to double exchange will also be discussed.

Fig. 6 shows the reciprocal susceptibility plotted against temperature for several of the compositions in the single-phase region of $Li_xCo_{(1-x)}O$. From an analysis of such susceptibility data above the antiferromagnetic Curie temperature, the values of $C$ (Curie constant/mole of Co) and $\Theta$ (paramagnetic Curie temperature) can be determined. These are

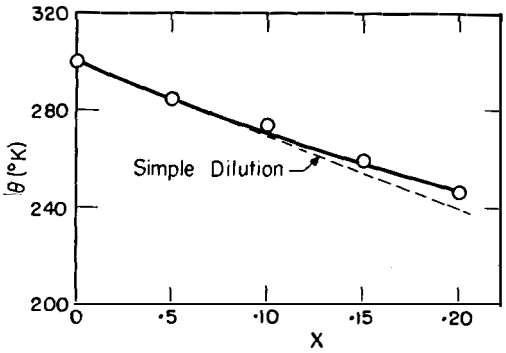


FIG. 8. Paramagnetic Curie temperature versus mole fraction of lithium.

RJ Technology Exhibit 2034
Apple Inc. v. RJ Technology LLC
IPR2023-01183, Page 8 of 13

plotted in Figs. 7 and 8. An examination of Fig. 7 shows that from $Li_{0.05}Co_{0.95}O$ to $Li_{0.20}Co_{0.80}O$ the Curie constant follows a smooth curve; however, for smaller lithium contents the data scatter considerably. Only the data from $0.05 < x < 0.20$ are to be considered as completely meaningful. The large scatter for $0 < x < 0.05$ is believed to be due to the presence of traces of cobalt metal. This point is discussed in Appendix I.

The data for $C$ will now be analyzed. In Appendix II it is shown that $C$ can be written

$$C = \frac{N\beta^2}{3k}\left[\frac{1-2x}{1-x}\cdot n_A{}^2 + \frac{x}{1-x}\cdot n_B{}^2\right],$$

where $\beta$ is the Bohr magneton, $N$ is Avogadro's number, and $n_A$ and $n_B$ are the magnitudes (in units of $\beta$) of the magnetic moments of the $Co^{+2}$ and $Co^{+3}$ ions respectively.

Using the experimental results at $x = 0.05$ and $x = 0.20$, the magnetic moments of $Co^{+2}$ and $Co^{+3}$ can be evaluated. These numbers are found to be

$$n_A{}^2 = 26.6,$$

$$n_B{}^2 = 4.4.$$

The solid curve in Fig. 7 was drawn using these values. Thus, for pure CoO we find the extrapolated value of $C$ to be 3.32. This value should be compared with $C = 3.21$ obtained by ELLIOT[19] and 3.42 obtained by SINGER.[20] It is now necessary to get an understanding of the magnitude of the magnetic moments of the two ions.

Before attempting to understand the magnitude of the magnetic moments of the specific ions in question, a brief survey of the situation might be helpful. In rare-earth salts it is generally found (samarium and europium are exceptions) that the magnetic moment is simply $g\beta\sqrt{J(J+1)}$, where $g$ is the Landé factor and $J$ is the total angular momentum quantum number (as determined for the free ion). In deriving the above-quoted value for the moment, it is assumed that all other $J$ values are so high energetically that their occurrence is negligible in the temperature range of measurement, i.e. the multiplet splitting is much greater than $kT$. On the other hand, if the multiplet splitting is much less than $kT$, the moment is found to be $\beta[4S(S+1)+L(L+1)]^{\frac{1}{2}}$.[21] This situation is not commonly discussed. Finally, in the iron-group dilute salts, it is generally found that the moment is best represented by $\beta\sqrt{4S(S+1)}$. In other words the orbital angular momentum $L$ is quenched.

As indicated above, $Co^{+2}$ has a moment of $\sqrt{26.6}\beta$. Pure CoO is cubic above room temperature. One therefore does not expect quenching of the orbital moment.[21] If the $Co^{+2}$ is assumed to be in a $^4F_{9/2}$ state (the ground state for the free ion), the above expressions for wide and narrow multiplet splitting give $\sqrt{43.5}\beta$ and $\sqrt{27}\beta$, respectively. From the excellent agreement between the latter value and the experimental one, it would appear that this is a case of narrow multiplet splitting. As evidence that this agreement is no coincidence, the data of SINGER[20] on NiO can also be cited. He finds the experimental moment of $Ni^{++}$ to be $\sqrt{21}\beta$, while the narrow multiplet moment is calculated to be $\sqrt{20}\beta$. In the calculation the free ion state ($^3F_4$) for $Ni^{+2}$ is used.

Unfortunately, the $Co^{+3}$ ion is not so simple. The narrow multiplet moment ($^5D_4$) is $\sqrt{30}\beta$, as compared to the experimental value of $\sqrt{4.4}\beta$. A possible explanation of this anomalously small moment may be found in the effect of the crystalline electric field on the $d$-electron levels. It is known[22] that the five $d$-levels of an ion in an octahedral site are split into a triplet and a doublet, the doublet being the higher energy level. The $d$-level configuration for the ion in the octahedral site of a cubic lattice is shown in Fig. 9a. If the

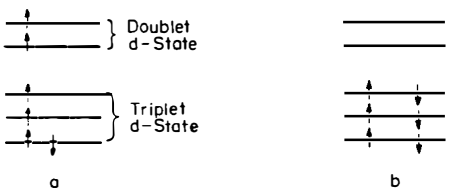


FIG. 9. $d$-Electron configuration for $Co^{+3}$.

crystalline fields cause sufficient splitting, it can become energetically advantageous for the electrons in the doublet level to drop into the triplet level and cancel the magnetic moment, as indicated in Fig. 9b. It only requires that the splitting is greater than the increase in exchange energy

RJ Technology Exhibit 2034
Apple Inc. v. RJ Technology LLC
IPR2023-01183, Page 9 of 13

accompanying the transfer. This interpretation would, of course, require zero moment for the $Co^{+3}$ instead of $\sqrt{4\cdot4}\beta$ as calculated. However, when the presence of monovalent lithium is considered, it is not surprising that this simple concept breaks down. $Co^{+3}$ ions in one set of surroundings may have a zero moment while in another set of surroundings they may have a non-zero moment due to insufficient splitting of the $d$ levels. Therefore the moment of $\sqrt{4\cdot4}\beta$ for $Co^{+3}$ should be considered as an average value over all $Co^{+3}$ ions. It is quite likely that this average moment will be a function of lithium content. However, considering the experimental error in susceptibility ($\pm1$ per cent), it does not seem fruitful to refine the model further.

It should be pointed out that such a behavior for $Co^{+3}$ is not uncommon. This ion is frequently found to be weakly paramagnetic or even diamagnetic.[23] If this model is accepted, it is necessary to indicate why it does not also occur in $Co^{+2}$. Because of the extra charge on $Co^{+3}$, the surrounding oxygen octahedron will be smaller, thereby increasing the perturbing effect on the $d$-levels due to the crystalline field.

Another significant quantity for the understanding of these materials is the paramagnetic Curie temperature $\Theta$. As $\Theta$ is essentially a measure of the Weiss internal field in the crystal, a qualitative interpretation can first be given. The replacement of a $Co^{+2}$ by $Li^{+1}$ has two effects. (1) It reduces by one the number of interactions for those Co ions neighboring to a $Li^{+1}$. (2) It replaces one $Co^{+2}$–$Co^{+2}$ interaction. Since $\Theta$ initially follows closely to a dilution law, the $Co^{+2}$–$Co^{+3}$ interaction must be approximately of the same magnitude and sign. As more lithium is introduced, $Co^{+3}$–$Co^{+3}$ interactions will arise. The number of such interactions will be proportional to the square of the $Li^{+1}$ concentration. Since $\Theta$ begins to deviate positively from the dilution law, we expect that the $Co^{+3}$–$Co^{+3}$ interaction is larger than the other interactions. Using the molecular field treatment given in Appendix II, a quantitative expression for $\Theta$ can be derived. $C_A$ and $C_B$, the Curie constants of the $A$ and $B$ ions for one formula weight of compound, are given by the following expressions:

$$C_A = \frac{N\beta^2(1-2x)}{3k}\cdot n_A{}^2 \text{ and } C_B = \frac{N\beta^2 x}{3k}\cdot n_B{}^2.$$

Substituting these in equation (1) of the Appendix

$$\Theta = -\frac{N\beta^2 n_A{}^2\gamma_{AA}}{3k}\left[1-\left\{2+\frac{n_B{}^2}{n_A{}^2}\left(1-\frac{2\gamma_{AB}}{\gamma_{AA}}\right)\right\}x+\right.$$
$$\left.+\frac{n_B{}^4}{n_A{}^4}\left(1+\frac{\gamma_{BB}}{\gamma_{AA}}-\frac{2\gamma_{AB}}{\gamma_{AA}}\right)\frac{x^2}{1-2x}\right].$$

The interaction constants, $\gamma$, are defined in the Appendix. This equation is seen to have all the qualitative features mentioned above. By fitting this equation at two points, the ratios $\gamma_{BB}/\gamma_{AA}$ and $\gamma_{AB}/\gamma_{AA}$ can be determined.

$$\frac{\gamma_{BB}}{\gamma_{AA}}\simeq 10 \qquad \frac{\gamma_{AB}}{\gamma_{AA}}\simeq 4.$$

Thus, all interaction in this phenomenological model are antiferromagnetic. This is especially to be noted in the case of the $\gamma_{AB}$ where the ferromagnetic double exchange might be anticipated. This point is discussed below.

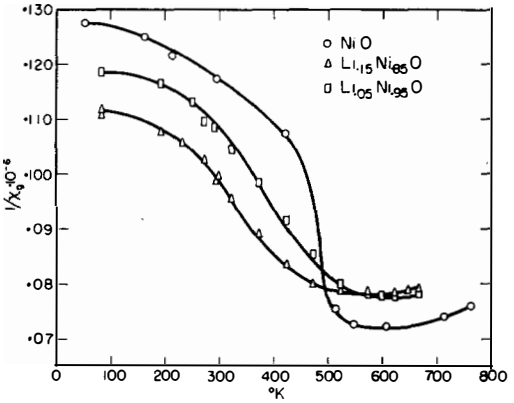


FIG. 10. Reciprocal susceptibility versus absolute temperature for $Li_xNi_{(1-x)}O$.

In Fig. 10 is plotted the $1/\chi$ versus $T$ curves for several compositions in the $Li_xNi_{1-x}O$ system. Again in the composition range studied this system does not exhibit ferromagnetism down to liquid-nitrogen temperature. Due to the work of PERAKIS *et al.*,[24] a separate study was made of $Li_{0.02}Ni_{0.98}O$.[25] The ferromagnetism reported by PARRAVANO for this composition was not confirmed. In the curves of the nickel system, the transition region from antiferromagnetism to paramagnetism becomes more gradual with increasing lithium concentration. This is similar to the results of

RJ Technology Exhibit 2034
Apple Inc. v. RJ Technology LLC
IPR2023-01183, Page 10 of 13

SHIMOMURA and TSUBOKAWA,[26] who replaced nickel by copper.

In the case of CuO, only a small amount of $Li^{+1}$ could be added. Except for the fact that $\chi$ is slightly higher, the lithium has not caused any significant change.

It remains to review the situation with regard to the double-exchange interaction. This interaction, as described by ZENER,[3] should result in a ferromagnetic coupling and metallic type conductivity. The present paper has shown that a ferromagnetic coupling does not arise. Furthermore, a previous paper[2] shows that the conductivity is semiconducting in type over the whole composition range.

The semiconductivity is interpreted as being due to a trapping of the positive holes caused by a local ionic polarization.[2] In a recent paper[27] it was shown that this trapping energy should decrease as the electronic polarizability of the ions increases. This can be understood qualitatively as follows. The introduction of a positive hole into the CoO lattice causes a certain amount of distortion. Part of the distortion occurs as a shift in the electron distribution of the ions and part as a shift in the ions themselves. It is only the ionic shift which is believed to contribute to the trapping.[28] Therefore, the introduction of an ion having a large electronic polarizability should decrease the trapping energy. It is possible that the trapping effect can disappear completely. If such a case happens, then a double-exchange type of interaction can occur; for this interaction requires that the electrons have no activation energy for motion. It is expected that the substitution of selenium or tellurium for oxygen in the present compound might be a case in point. This substitution is now being attempted.

## APPENDIX I

### *Effect of Metallic Cobalt on Magnetic Data*

The large scatter of the magnetic data for small lithium content will now be examined. First, it must be pointed out that duplicate samples of the same nominal composition show significant differences in $C$ and $\chi$. Secondly, this is not due to scatter in the magnetic measurements. Furthermore, X-rays show no observable difference between samples with widely different values of $C$. It is observed that all the scatter is on the high side of the theoretical curve. Also for a particular value of $x$ the $\chi$ is found to be higher the higher the $C$. This leads to a consideration of the presence of small quantities of free cobalt metal. The susceptibility for a sample containing a small amount of free cobalt can be written

$$\chi_g(\text{exp}) = (1-f)\chi_g + f\frac{I_{Co}}{H} \tag{1}$$

where $\chi_g$ = value of susceptibility for pure sample ($f = 0$), $\chi_g(\text{exp})$ = measured value per $g$, $f$ = weight fraction of free cobalt, and $I_{Co}$ = magnetization of Co/g.

As the $Li_{0.002}Co_{0.998}O$ samples show the widest deviation, they will be examined in detail. It will be assumed that sample No. 2 (see below), with a Curie constant almost on the theoretical curve, has $f = 0$. Then, examining sample No. 1, the difference in $\chi$ and $C$ will be attributed to free cobalt. Using (1) $f$ can be calculated from the following data:

| | $\chi_g$(exp)(at 400°K) | $C_g$(Curie constant/g) |
|---|---|---|
| No. 1 | $76\times10^{-6}$ | 0·071 |
| No. 2 | $64\times10^{-6}$ | 0·045 |

It is found that $f \sim 10^{-3}$ or 0·1 per cent free cobalt. Such amounts could not be detected by X-rays. As a check, the amount of free cobalt needed to affect $C$ can be calculated in the following way:

$$\chi = \frac{(1-f)C_g}{T+\Theta} + f\frac{I_{Co}}{H}.$$

The equation can then be put in the standard form for paramagnetic substances:

$$\chi = \frac{(1-f)C_g + f\frac{I_{Co}}{H}(T+\Theta)}{T+\Theta}.$$

Then

$$C_{\text{eff}} = (1-f)C_g + f\frac{I_{Co}}{H}(T+\Theta).$$

Using the data above, $f \sim 0{\cdot}2$ per cent. Therefore, free cobalt appears to be a satisfactory explanation.

## APPENDIX II

### *Molecular Field Treatment*

In order to interpret the results of the magnetic measurements, it is necessary to derive an expression for the susceptibility above $T_c$ in terms of the lithium concentration and the various interaction parameters. A molecular field treatment will be given here. As the basis for such a treatment is well known,[29] it will not be discussed here.

Consider a f.c.c. lattice containing $x Co^{+3}$ ions (designated $B$), $(1-2x)Co^{+2}$ ions (designated $A$), and $x$ Li ions randomly distributed. Previous work[2] on the electrical conductivity of these systems indicates that random distribution of $Co^{+2}$ and $Co^{+3}$ is a good assumption. Nearest-neighbor and next-nearest-neighbor interactions will be treated. The interaction between an

RJ Technology Exhibit 2034
Apple Inc. v. RJ Technology LLC
IPR2023-01183, Page 11 of 13

ion—an $A$ ion, for example—with its neighbors will be assumed to be of the form

$$-2\alpha_{Ai}\bar{J}_A\sum_i\bar{J}_i,$$

where $\bar{J}$ represents the total angular momentum quantum number and $i$ is summed over all nearest and next-nearest neighbors. (It is recognized that the double-exchange interaction can not be put in this form.[30] However, for this phenomenological treatment the $Co^{+2}$–$Co^{+3}$ will be expressed in this way.) The standard approximation is to replace $\bar{J}$ by an appropriate average. Thus

$$V_A=-2\bar{J}_A\alpha^1_{AA}Z_1(1-2x)\frac{I_A}{N(1-2x)g\beta}+$$
$$+\alpha^1_{AB}Z_1x\frac{I_B}{Nxg\beta}+\alpha^2_{AA}Z_2(1-2x)\frac{I_A}{N(1-2x)g\beta}+$$
$$+\alpha^2_{AB}Z_2x\frac{I_B}{Nxg\beta}.$$

Here $\alpha^1_{AA}$ = nearest-neighbor $A$–$A$ interaction, $\alpha^2_{AA}$ = next-nearest-neighbor $A$–$A$ interaction, $Z_1$ = no. of nearest neighbors, $Z_2$ = no. of next-nearest neighbors and $I_A$ = magnetization of the $A$ ions.

In the above equation, the average value of $J_A$ is replaced by

$$\frac{I_A}{N(1-2x)g\beta}$$

Now

$$V_A=\frac{-2}{Ng^2\beta^2}[Z_1(\alpha^1_{AA}I_A+\alpha^1_{AB}I_B)+Z_2(\alpha^2_{AA}I_A+$$
$$+\alpha^2_{AB}I_B)\bar{M}_A,$$

where $\bar{M}_A=g\beta\bar{J}_A$ is the magnetic moment of an $A$ ion. From this equation one finds the effective field for the $A$ ion to be

$$H^{\text{eff}}_A=\frac{2}{Ng^2\beta^2}[Z_1(\alpha^1_{AA}I_A+\alpha^1_{AB}I_B)+$$
$$+Z_2(\alpha^2_{AA}I_A+\alpha^2_{AB}I_B)].$$

The effective field for a $B$ ion is found by simply interchanging indices. We now use the Curie–Weiss law, which states that

$$I=\frac{C}{T}(H_0+H^{\text{eff}}),$$

where $C$ is the Curie constant and $H_0$ is the applied field. Thus,

$$I_A=\frac{C_A}{T}[H_0+\gamma_{AA}I_A+\gamma_{AB}I_B]$$

$$I_B=\frac{C_B}{T}[H_0+\gamma_{BB}I_B+\gamma_{AB}I_B],$$

where

$$\gamma_{AA}=Z_1\alpha^1_{AA}+Z_2\alpha^2_{AA}.$$

Solving for $I_A$ and $I_B$

$$I_A=\frac{H_0\left[\frac{T}{C_B}-\gamma_{BB}+\gamma_{AB}\right]}{\left(\frac{T}{C_A}-\gamma_{AA}\right)\left(\frac{T}{C_B}-\gamma_{BB}\right)-\gamma_{AB}^2}$$

$$I_B=\frac{H_0\left[\frac{T}{C_A}-\gamma_{AA}+\gamma_{AB}\right]}{\left(\frac{T}{C_A}-\gamma_{AA}\right)\left(\frac{T}{C_B}-\gamma_{BB}\right)-\gamma_{AB}^2}.$$

As

$$1/\chi=\frac{H_0}{I_A+I_B},$$

it can now be determined. To a second approximation this result can be written

$$\frac{1}{\chi}=\frac{T-(\gamma_{BB}C_B+\gamma_{AA}C_A)+\frac{C_AC_B(\gamma_{AA}+\gamma_{BB}-2\gamma_{AB})}{C_A+C_B}}{C_A+C_B}$$

using the form

$$1/\chi=\frac{T+\Theta}{C},$$

where

$$C=C_A+C_B \text{ and } \Theta$$
$$=-(\gamma_{BB}C_B+\gamma_{AA}C_A)+\frac{C_AC_B(\gamma_{AA}+\gamma_{BB}-2\gamma_{AB})}{C_A+C_B}.$$

It is easily seen that the Curie constant per formula weight can be written

$$C_{\text{F.W.}}=\frac{N\beta^2}{3k}[(1-2x)N_A^2+xN_B^2].$$

RJ Technology Exhibit 2034
Apple Inc. v. RJ Technology LLC
IPR2023-01183, Page 12 of 13

To convert this expression to Curie constant per mole of cobalt ion, it is necessary only to divide by the factor $(1-x)$.

## REFERENCES


1. JOHNSTON W. D. and HEIKES R. R. *J. Amer. Chem. Soc.* **78,** 3255 (1956).
2. HEIKES R. R. and JOHNSTON W. D. *J. Chem. Phys.* **26,** 582 (1957).
3. ZENER C. *Phys. Rev.* **82,** 403 (1951).
4. GREENWALD S. *Acta Cryst.* **6,** 396 (1953).
5. TOMBS N. C. and ROOKSBY H. P. *Nature Lond.* **165,** 442 (1950).
6. GREENWALD S. and SMART J. S. *Nature Lond.* **166,** 523 (1950).
7. SHULL C. G. and SMART J. S. *Phys. Rev.* **76,** 1256 (1949).
8. LI Y. Y. *Phys. Rev.* **100,** 627 (1955).
9. KEFFER F. and O'SULLIVAN W. *Phys. Rev.* **108,** 637 (1957).
10. CORLISS L., ELLIOTT N. and HASTINGS J. *Phys. Rev.* **104,** 924 (1956).
11. LOEB A. L. and GOODENOUGH J. B. Conference on Magnetism and Magnetic Materials, Boston, Oct. 1956.
12. ROTH W. L. *Bull. Amer. Phys. Soc.* **2,** 119 (1957).
13. SHIMOMURA Y. *J. Japan Inst. Metals* **17,** 421 (1951).
14. BROWNLEE L. D. and MITCHELL E. W. J. *Proc. Phys. Soc.* B **65,** 710 (1952).
15. ELLESTAD R. B. and BABBITT B. R. U.S. Patent 2,545,424.
16. KLUG H. P. and ALEXANDER L. E. *X-ray Diffraction Procedures.* John Wiley and Sons, New York (1954).
17. BONGERS P. F. Thesis, Univ. of Leiden, July 4, 1957.
18. DYER L. D., BORIE B. S. Jr. and SMITH G. P. *J. Amer. Chem. Soc.* **76,** 1479 (1954).
19. ELLIOT N. *J. Chem. Phys.* **22,** 1924 (1954).
20. SINGER J. R. *Phys. Rev.* **104,** 928 (1956).
21. VAN VLECK J. H. *Electric and Magnetic Susceptibilities.* Oxford University Press (1932).
22. VAN VLECK J. H. *J. Chem. Phys.* **3,** 807 (1935).
23. COSSEE P. *Rec. Trav. Chim. Pays-Bas* **75,** 1089 (1956).
24. PERAKIS N., SERRES A., PARRAVANO G. and WUCHER J. *C.R. Acad. Sci., Paris* **242,** 1275 (1956).
25. JANUSZ T. P., HEIKES R. R. and JOHNSTON W. D. *J. Chem. Phys.* **26,** 973 (1957).
26. SHIMOMURA Y. and TSUBOKAWA I. *J. Phys. Soc. Japan* **9,** 19 (1954).
27. ZENER C. and HEIKES R. R. Conference on Magnetism and Magnetic Materials, 1956.
28. MOTT N. F. and GURNEY R. W. *Electronic Processes in Ionic Crystals* p. 87. Oxford University Press (1940).
29. SMART J. S. *Rev. Mod. Phys.* **25,** 327 (1953).
30. ANDERSON P. W. and HASEGAWA A. *Phys. Rev.* **100,** 675 (1955).


RJ Technology Exhibit 2034
Apple Inc. v. RJ Technology LLC
IPR2023-01183, Page 13 of 13